



Ultra-faint dwarfs and dwarf-spheroidal galaxies: the Andromeda satellites

G. Coppola¹, F. Cusano², G. Clementini², V. Ripepi¹, I. Musella¹, L. Federici²,
M. Marconi¹, L. Di Fabrizio³, A. Ferguson⁴, M. Tosi², F. Fusi Pecci², R. Contreras²,
M. Dall’Ora¹, and A. Garofalo^{2,5}

¹ INAF – Osservatorio Astronomico di Capodimonte, Salita Moiarriello 16, I-80131 Napoli, Italy

² INAF – Osservatorio Astronomico di Bologna, Via Ranzani 1, I-40127 Bologna, Italy

³ INAF – Centro Galileo Galilei & Telescopio Nazionale Galileo, E-38700 S. Cruz de La Palma, Spain

⁴ SUPA – Institute for Astronomy, University of Edinburgh, Royal Observatory, Blackford Hill, Edinburgh EH9 3HJ

⁵ Dipartimento di Astronomia, Università di Bologna, Via Ranzani 1, I-40127 Bologna, Italy

Abstract. We present preliminary results on the study of the variable stars and the stellar population of the Andromeda IX (And IX) and the Andromeda X (And X) companions of M31. The study is based on g' , r' time series photometry that we obtained as part of our ESO Large Program 186.D-2013 at the Gran Telescopio Canarias (GTC, P.I. G. Clementini). More than twenty RR Lyrae stars were discovered in each galaxy and well sampled and accurate light curves were obtained. The color magnitude diagrams (CMDs) obtained by stacking the 23 pairs of g' , r' exposures available for each galaxy are ~ 2 mag deeper than those presently available in the literature. And IX and And X have prominent red giant branches and clearly visible horizontal branches, although both galaxies are rather contaminated by field stars. The CMD of And IX is well fitted by the mean ridge lines of the metal-poor ($[Fe/H]=-2.2$ dex) Galactic globular cluster NGC 2419. The steepness of And X’s red giant branch seems to suggest a metallicity even lower than NGC 2419.

Key words. galaxies: dwarf-galaxies: individual (And IX-And X)-stars: distances-stars: variables:other

1. Introduction

The number of dwarf spheroidal galaxies (dSphs) and ultra-faint dwarfs (UFDs) surrounding the Milky Way (MW) and the Andromeda (M31) galaxies has increased in the last years thanks to the wide-field photometric survey of the MW halo by the Sloan Digital Sky Survey (SDSS; see, e.g. Belokurov

et al. 2007, 2010) and the panoramic views of Andromeda being obtained by the Isaac Newton and the Canada-France-Hawaii telescope surveys (Ferguson et al. 2002; Ibata et al. 2007; McConnachie et al. 2009).

M31 dSphs and UFDs have the same morphological properties of their MW counterparts: they often present an irregular shape

likely due to the tidal interaction with the Andromeda galaxy; they are fainter ($\mu_V > 28 \text{ mag/arcsec}^2$) than previously known *classic* dSphs; and they show high mass-to-light ratios (McConnachie 2012).

In the absolute magnitude versus half-light radius plane (Belokurov diagram, Belokurov et al. 2007, see Figure 1 of Clementini et al. 2012 for an updated version of this diagram) the M31 satellites are located at the faintest end of the distribution of their M31 *classical* companions and on the extension to brighter luminosities of the MW UFDs. Their stellar content is not well known, since the CMDs presently available generally cover only the brightest portion of the red giant branch and only in a few cases reach magnitudes below the horizontal branch (Ibata et al. 2007; Collins et al. 2009; Letarte et al. 2009).

We are carrying out the systematic study of a number of the M31 UFDs and dSphs, using both space- and ground-based facilities, to characterize the stellar populations as well as the variable stars of these systems, and get insights on the star formation history and the merging episodes that led to the assembling of the M31 halo. Here, we present results for And IX (Zucker et al. 2004) and And X (Zucker et al. 2007) that were observed with the Gran Telescopio Canarias (GTC) as part of our ESO Large Program 186.D-2013 (P.I. G. Clementini).

2. Observations and data reduction

g' , r' time-series photometry of And IX was obtained with the OSIRIS camera at the GTC during nine nights in October-November 2010. The observations of And X were obtained in nine nights from October 2010 to August 2011. In both cases the observations were organized in 23 elementary observing blocks (OBs) of about 1 hr, each corresponding to a pair of [g' , r'] exposures of 26.7 min per filter. To avoid sky saturation, each 26.7 min exposure was split into 8 sub-exposures of 200 sec. All OBs, were executed under seeing better than 1.0 arcsec, and using a 2×2 binning giving an actual scale of 0.25 arcsec/pixel. We performed PSF photometry using the

Table 1. Internal errors of the g' , r' single-epoch photometry at the HB magnitude level of And IX and And X.

Galaxy	HB level (g') (mag)	$\sigma_{g'}$ (mag)	$\sigma_{r'}$ (mag)
And IX	25.50	0.04	0.04
And X	25.00	0.03	0.04

DAOPHOT IV/ALLSTAR/ALLFRAME packages (Stetson 1987; Stetson & West 1994). A reference image was built for each galaxy by averaging all the available frames and a source catalogue was extracted from the stacked image. The source list was then passed to ALLFRAME, in order to perform the homogeneous photometry of all images simultaneously, thus obtaining g' and r' catalogues in instrumental magnitude. We then averaged the magnitudes of each 8 sub-images dataset to obtain the 23 epoch data (in both g' and r' bands) used to study the variable stars. Typical internal errors of the single-epoch g' , r' data for stars at the horizontal branch (HB) magnitude level are provided in Table 1 for both galaxies, separately.

For the photometric calibration of the data we used as local standards about 100 stars observed in the field of the M31 satellites by the SDSS with photometric accuracy $\sigma_{r'_{SDSS}} < 0.1 \text{ mag}$. The final calibrated catalogues contain positions, robust intensity-weighted mean g'_{SDSS} and r'_{SDSS} magnitudes, and weighted average values of the χ and *Sharp* parameters (Stetson 1987) for all sources measured in the total FOVs of each galaxy.

3. Color magnitude diagram

The 23-epoch g' , r' data of And IX and And X (cut according to the *Sharp* and χ values described at the end of Section 2) were further averaged to obtain deep CMDs for the two galaxies, these are shown in Figures 1 and 2. In both figures the left panels show the CMDs from stars in the area enclosed by an ellipse having the major axis equal to the galaxy half-light radius (2.50 arcmin, and 1.6

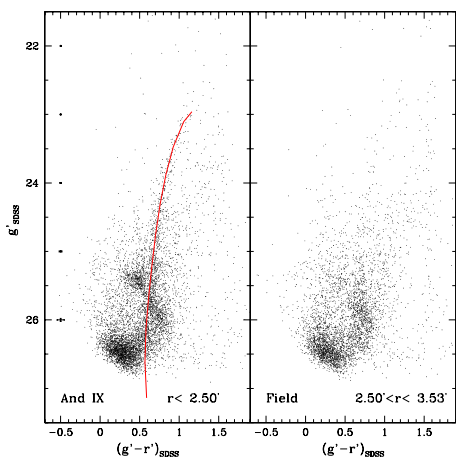


Fig. 1. CMD of the And IX galaxy, based on the average PSF photometry of the 23 single-epoch data. *Left panel:* CMD of stars belonging to an area inside the ellipse having the major axis equal to the And IX half-light radius; the red line shows the fiducial sequence of the Galactic GC NGC 2419 from An et al. (2008); *Right panel:* CMD of the foreground/background field stars. The sky area covered by two panels is the same. The error-bars in the left panel show the internal precision of the photometry at different magnitude levels.

arcmin for And IX and And X, respectively) and inferring the minor axis from the axial ratio (where half-radii and axial ratios were taken from Zucker et al. 2004, 2007). The right panels in both figures show instead the CMDs of foreground/background field stars in an external area of the same size of the area enclosed inside the elliptical regions. Our CMDs reach $g'_{SDSS} \sim 27.3$ mag and $g'_{SDSS} \sim 26.0$ mag for And IX and And X, respectively.

The red giant branch (RGB) of And IX is clearly visible in Figure 1, as well as the horizontal branch (HB, $g'_{SDSS} \sim 25.3$ mag) even if contaminated by field stars. A residual of the galaxy RGB can still be seen in the CMD in the right panel of Figure 1, thus showing that And IX extends beyond its half-light radius. And IX is located close to the M31 disk and in a region crossed by several streams. This explains the complex structure of the field star CMD, and the strong contamination affecting the galaxy

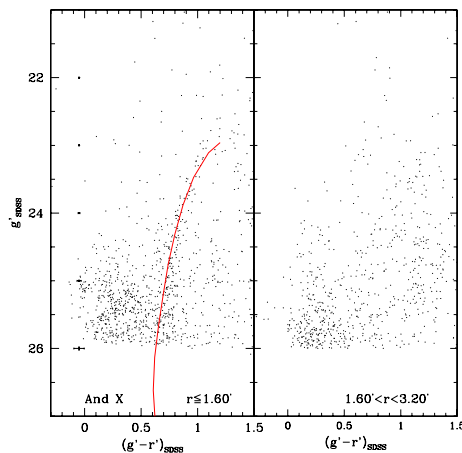


Fig. 2. Same as in Figure 1, but for And X.

HB. We have fitted the RGB of And IX to the fiducial sequence (red line in the left panel of Figure 1) of the Galactic globular cluster (GC) NGC 2419 ([Fe/H]=-2.2 dex on the Carretta et al. (2009) metallicity scale) taken from An et al. (2008). The good match we have obtained confirms that the stellar population of And IX resembles that of a metal poor GC like NGC 2419.

Figure 2 shows the CMD of And X obtained in the present study. Although And X is much sparsely populated than And IX the galaxy RGB and the HB ($g'_{SDSS} \sim 25.0$ mag) are still distinguished. As with And IX the red line in the left panel of Figure 2 corresponds to the fiducial line of NGC 2419. However, the match to NGC 2419 is less satisfactory as the RGB of And X appears to be steeper and require lower metallicity than NGC 2419 to be properly matched.

4. Variable stars

We have detected and obtained well sampled light curves for more than twenty variables in each of the two galaxies. They are mainly RR Lyrae stars. Figures 3 and 4 show the g_{SDSS} -band light curves of a fundamental-mode (upper) and first-overtone (bottom) RR Lyrae star of And IX and And X, respectively. The peri-

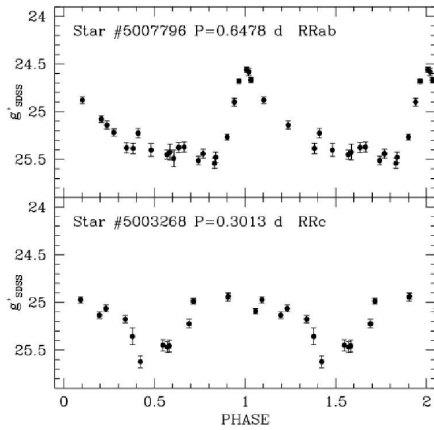


Fig. 3. g'_{SDSS} -band light curve for fundamental-mode (RRab; top panel) and first-overtone (RRc; bottom panel) RR Lyrae star in the And IX dSph. Period and RR Lyrae type are labeled

ods of the variables are reported in each panel. The error-bars are representative of the uncertainty of each phase point. This uncertainty is below 0.1 mag even at minimum light.

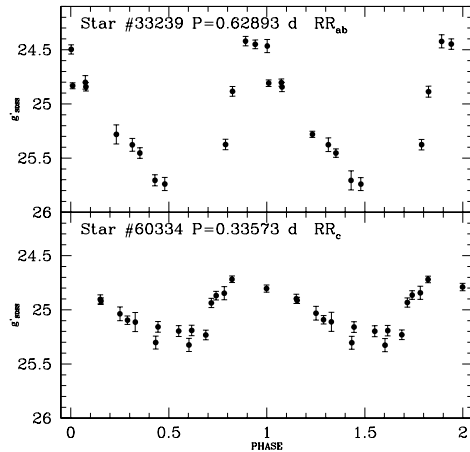


Fig. 4. Same as Figure 3, but for an RRab and an RRc star in And X.

5. Summary

We have obtained time series photometry of 5 dwarf spheroidal and ultra-faint dwarf satellites of M31 with the Gran Telescopio Canarias as part of the ESO Large Program 186.D-2013 (*Stellar Archaeology in the M31 halo: variable stars and stellar populations in the And IX, And X, And XXIV, and And XV dwarf spheroidal galaxies*, P.I. G. Clementini). Observations have already been completed for all the five targets. The PSF photometry with DAOPHOT/ALLSTAR/ALLFRAME of the And IX and And X datasets has been completed. In particular we reach $g'_{SDSS} \sim 27.3$ mag and $g'_{SDSS} \sim 26.0$ mag for And IX and And X, respectively. These is about 2 magnitudes deeper than presently available in literature (Ibata et al. 2007; Collins et al. 2009; Letarte et al. 2009). More than 20 RR Lyrae stars were identified in each galaxy, for which we have obtained well sampled light curves and accurate periods and mean magnitudes. A detailed study of the stellar populations and variable star content of And IX and And X is in progress, to derive constraint on their distance and star formation history.

References

- An, D., et al. 2008, ApJS, 179, 326
- Belokurov, V., et al. 2007, ApJ, 654, 897
- Belokurov, V., et al. 2010, ApJ, 712, L103
- Carretta, E., et al. 2009, A&A, 508, 695
- Clementini, G., Cignoni, M., Contreras Ramos R. et al. 2012, ApJ, 756, 108
- Collins, M. L. M., et al. 2009, MNRAS, 396, 1619
- Ferguson, A. M. N., et al. 2002, AJ, 124, 1452
- Ibata, R., et al. 2007, ApJ, 671, 1591
- Letarte, B., et al. 2009, MNRAS, 400, 1472
- McConnachie, A. W., et al. 2009, Nature, 461, 66
- McConnachie, A. W. 2012, AJ, 144, 4
- Stetson, P. B. 1987, PASP, 99, 191
- Stetson, P. B., & West, M. J. 1994, PASP, 106, 726
- Zucker, D. B., et al. 2004, ApJ, 612, L121
- Zucker, D. B., et al. 2007, ApJ, 659, L21